Initializing a permutation-invariant quantum error-correction code

Chunfeng Wu, Yimin Wang, Chu Guo, Yingkai Ouyang, Gangcheng Wang, and Xun-Li Feng

Initializing a permutation-invariant quantum error correction code

Chunfeng Wu,[1, 2, *] Yimin Wang,[3, 4, †] Chu Guo,[2] Yingkai Ouyang,[2, 5] Gangcheng Wang,[6] and Xun-Li Feng[7, ‡]

[1]*Science and Mathematics, Singapore University of Technology and Design, 8 Somapah Road, Singapore 487372*
[2]*Pillar of Engineering Product Development, Singapore University*
of Technology and Design, 8 Somapah Road, Singapore 487372
[3]*Communications Engineering College, Army Engineering University, Nanjing, Jiangsu 210007, China*
[4]*Shanghai Key Laboratory of High Temperature Superconductors, Shanghai 200444, China*
[5]*Centre for Quantum Technologies, National University of Singapore, 3 Science Drive 2, Singapore 117543*
[6]*Center for Quantum Sciences and School of Physics,*
Northeast Normal University, Changchun 130024, China
[7]*Department of Physics, Shanghai Normal University, Shanghai 200234, China*
(Dated: December 26, 2018)

Recently, there has been growing interest in using quantum error correction in practical devices. A central issue in quantum error correction is the initialization of quantum data into a quantum error correction code. Most studies have concentrated on generating quantum codes based on their encoding quantum circuits. However, this often leads to a large number of steps required in the initialization, and hence this process can be prone to errors. The purpose of this work is to demonstrate that permutation-invariant quantum error correction codes can be created with high fidelity by exploiting their underlying symmetry. The code is initialized on multiple qubits that mutually interact, or are themselves coupled to a quantum harmonic oscillator. We show that the so-called selective resonant interaction is derivable on such physical systems. By utilizing the selective resonant interaction, these highly symmetric codes may be rapidly generated with excellent fidelity. We also discuss the potential of initializing permutation-invariant quantum error correction codes based on the state-of-art experimental techniques.

I. INTRODUCTION

To unlock the powers promised by quantum technologies for either quantum communication, quantum simulation, or quantum computation, it is essential to reliably initialize quantum information with protection from the environment's decohering effects. One way to make quantum information more robust is to encode it into a quantum error correction code (QECC). Once this quantum information has been encoded, it becomes possible, at least in principle, to mitigate the decohering effects that the quantum information experiences. Ever since of the proof of the possibility of quantum error correction [1–3], there has been extensive research on various types of QECCs, such as the surface codes [4] and many others too numerous to mention. However, initializing quantum states in QECCs remains challenging in practical devices. In this paper, we address the possibility of initializing QECCs with high fidelity.

Initializing quantum states in QECCs is necessary to realize the potential of quantum error correction in making quantum information more robust. For example, a single qubit can be protected by introducing $N - 1$ additional qubits, and applying an operation that entangles all the N qubits. If the now entangled qubits reside in a QECC of distance $2t + 1$, any errors on any t of the qubits can be corrected [5]. Most studies have concentrated on

initializing quantum codes based on their encoding quantum circuits, the circuits of which can be decomposed in terms of single-qubit and two-qubit gates. However, the number of these gates required often cannot be small [6–9]. Since every gate invariably incurs some amount of error, over time, the error builds up, and this leaves the initialization of quantum code that require many gates to be error-prone. This problem has motivated the use of different approaches to shorten the required evolution time in the generation of multi-qubit entangled states. Recently, a scheme based on ultrafast controlled phase gate and the principle of pairwise cluster state generation has been proposed, which utilizes ultrastrong qubit-resonator coupling to implement single-qubit and two-qubit quantum operations, and hence reduces the times required for the generation of QECCs [10]. Others have also explored special quantum operations to minimize the steps of evolution needed for creating multipartite entangled states [11–15].

Of the many QECCs that can be used, we focus our attention on permutation-invariant QECCs, which remain unchanged under the swapping of any of their underlying subsystems. Such codes can have a distance that grows as a square root of the number of underlying subsystems, and lie within the ground state space of any Heisenberg ferromagnet. Because of this and the fact that Heisenberg ferromagnets are naturally abundant in nature and can be made via engineered exchange interactions, these codes might be attractive for use in quantum storage. Although considerable research has been devoted to the construction of these codes and proving their quantum error correction properties [16–21], much

*Electronic address: chunfeng_wu@sutd.edu.sg
†Electronic address: vivhappyrom@gmail.com
‡Electronic address: xlfeng@shnu.edu.cn

less attention has been paid to that of initializing states within their codespace. Because permutation-invariant QECCs do not have an obvious stabilizer structure, their encoding quantum circuits remain unexplored.

In this paper, we investigate the initialization of a nine-qubit permutation-invariant QECC that encodes a single qubit and can correct any single qubit error. We show how any qubit can be encoded into this code using only a few steps of system evolution. This QECC can be seen as a variant of Ruskai's code [16]. The physics of how our scheme works is based on a controllable interaction which can be derived in two physical systems. When the so-called large detuning constraint holds, our scheme achieves a selective resonant interaction, which effectively induces Rabi oscillations between pairs of chosen basis states in the symmetric subspace. The natural unitary dynamics can be induced by the system Hamiltonian describing qubit-qubit coupling or qubit-resonator coupling. In view of the state-of-the-art techniques, our QECC scheme is possibly implementable with superconducting charge qubits coupled by a common inductance or embedded in a transmission line resonator.

This paper is organized as follows. In Sec. II, we investigate a physical system with coupled qubits and show that the system Hamiltonian leads to the selective resonant interaction. In Sec. III, we investigate the generation of a nine-qubit permutation invariant quantum code via a multi-step evolution of the system. In Sec. IV, we discuss the effect of decoherence on the creation of the 9-qubit QECC. In Sec. V, we present another system Hamiltonian of qubit-resonator coupling and derive a transformed Hamiltonian which also gives rise to the selective resonant interaction, followed by the exploration of the initialization of the 9-qubit QECC. Finally, we conclude this paper with discussions in Sec. VI.

II. THE SELECTIVE RESONANT INTERACTION FROM QUBIT-QUBIT COUPLING

We consider a quantum system of N identical qubits coupled to each other, where the system Hamiltonian is of the following form,

$$H = \sum_i \frac{\hbar\epsilon}{2}\sigma_z^i + \sum_i \frac{\hbar\Delta}{2}\sigma_x^i + \sum_{i<j} \hbar\Omega\sigma_x^i\sigma_x^j \quad (1)$$

where ϵ and Δ are the parameters describing the energy of each qubit, σ_x^i and σ_z^i describe Pauli matrices for i-th qubit and Ω is the coupling strength between qubits i and j.

Denote two states $|+_j\rangle$ and $|-_j\rangle$ of the j-th qubit, where $\sigma_x^j|+_j\rangle = |+_j\rangle$ and $\sigma_x^j|-_j\rangle = -|-_j\rangle$. Define $|N,n\rangle$ to be the Dicke state with n qubits in the excited state $|+_j\rangle$ and $N-n$ qubits in the ground state $|-_j\rangle$. One can easily show that $|N,n\rangle$ is an eigenstate of $\sum_i \frac{\hbar\Delta}{2}\sigma_x^i + \sum_{i<j}\hbar\Omega\sigma_x^i\sigma_x^j$ with energy $E_n =$ $\frac{2n-N}{2}\hbar\Delta - \hbar\Omega(N - 4n^2 + 4Nn - N^2)$. The energy gap $d_n = E_{n+1} - E_n$ between two adjacent energy levels can be written as $d_n = \hbar\Delta - 2\hbar\Omega(N - 2n - 1)$. By tuning the parameters Δ and Ω, one can adjust the values of d_n. We are interested in the regime where exactly one of the energy gaps is zero and the remaining gaps are non-zero, so that $d_{n_0} = 0$ for some n_0 and $d_n \neq 0$ for all $n \neq n_0$. In this case, the effective coupling strengths of the transitions $|N,n\rangle \leftrightarrows |N, n+1\rangle$ for all n is given by $g_n^{\text{eff}} = \hbar\epsilon\sqrt{(N-n)(n+1)}/2$ and can be tuned via the parameter ϵ. When the energy gaps d_n are much larger than g_n^{eff} for all $n \neq n_0$, we say that the large detuning constraint is satisfied, and the system's evolution can be described by the following selective resonant interaction,

$$H_{\text{eff}} = g_{n_0}^{\text{eff}}\big(|N,n_0\rangle\langle N, n_0 + 1| + |N, n_0 + 1\rangle\langle N, n_0|\big), \quad (2)$$

because, in this case, the other transitions corresponding to $n \neq n_0$ are dispersively coupled. This is the well-known selective resonant interaction.

We numerically calculate the population of $|N,n\rangle$ by taking $N = 9$ and $n = 0, \cdots, 9$ as examples when the system evolves from different initial states. The system parameters are selected in order to fulfil the large detuning constraint. Specifically, $\Omega/2\pi = 500\text{MHz}$ and $\epsilon = 0.03\Omega$, and Δ is changing according to the initial states. As illustrated in Fig. 1, there are almost perfect oscillations between the neighboring states $|9,n\rangle$ and $|9, n+1\rangle$, and nearly zero populations in the rest of the states.

Since our scheme requires the adjustment of Δ, one practical problem is how this adjustment may change the actual dynamics in the system via affecting the system's energy levels. The variation of energy levels is usually described by Landau-Zener transitions in which the variation is expressed as a linear function of time [22]. Here we suppose $\epsilon = \epsilon_0(1 - 2t/T)$ where T is evolution time. Since our scheme is based on the selective resonant interaction, the required evolution time is proportional to the inverse of g_n^{eff} and depends on ϵ. In our prior analysis, the energy levels are constant with respect to time, and hence time-variations in the energy levels may adversely affect our scheme. To resolve this issue, we approximately make the energy levels time-independent by periodically adjusting ϵ_0. To see how this works, first recall that the time-dependent energy levels arise from using a fixed ϵ_0. Now we divide the entire required time interval to many subintervals, and vary ϵ_0 accordingly. The time-dependent energy levels are described by a linear function of time, and can be approximated with a piecewise continuous constant function, which is constant on every time subinterval. By suitably adjusting ϵ_0 at the beginning of each time subinterval, the resultant energy level can approximate that of a continuous constant function for the entire time period. We provide numerical results when the system evolves initially from $|9,0\rangle$ for a time period of $[0, \pi/(2g_0^{\text{eff}})]$ by utilizing 10 subintervals in Table I. We use the constant function to determine evolution time and let the system evolve according to the time-dependent Hamiltonian on every time subinterval.
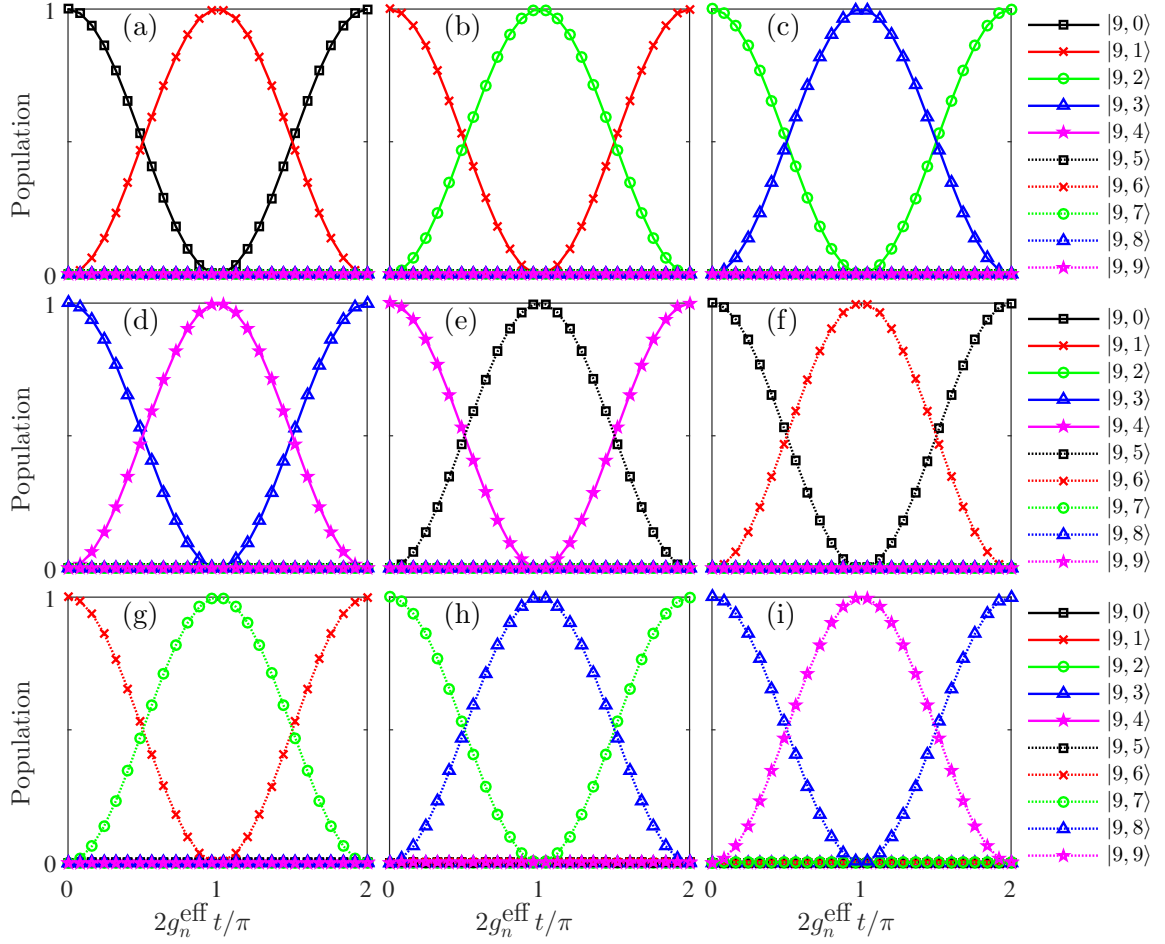
FIG. 1: Population of $|9, n\rangle$ (where $n = 0, \cdots, 9$) with initial states prepared in (a) $|9, 0\rangle$, (b) $|9, 1\rangle$, (c) $|9, 2\rangle$, (d) $|9, 3\rangle$, (e) $|9, 4\rangle$, (f) $|9, 5\rangle$, (g) $|9, 6\rangle$, (h) $|9, 7\rangle$, and (i) $|9, 8\rangle$, respectively by appropriately selecting parameters. Time t's are dependent on g_n^{eff} where $n = 0$ for (a), $n = 1$ for (b), $n = 2$ for (c), $n = 3$ for (d), $n = 4$ for (e), $n = 5$ for (f), $n = 6$ for (g), $n = 7$ for (h), and $n = 8$ for (i).

The numerical results show that the change of energy levels only slightly affects our scheme by using the approximation. It is reasonable to expect further improvement if the number of subintervals is increased.

III. INITIALIZING A NINE-QUBIT PERMUTATION INVARIANT QUANTUM CODE

With controllable parameters to implement the selective resonant interaction, a permutation-invariant QECC can be generated. We now elaborate on the initialization of the QECC which is a nine-qubit state. Let the system evolve from $|9, 0\rangle$ according the following steps by fixing the parameters $\Omega/2\pi = 500$MHz and $\epsilon = 0.03\Omega$ while adjusting Δ.

Step 1. Initially, we prepare the system in the state $|9, 0\rangle$ and apply the Hamiltonian with $\Delta = 16\Omega$ to ensure selective resonance between the states $|9, 0\rangle$ and $|9, 1\rangle$. As shown in Fig. 1 (a) we obtain

nearly perfect oscillations between the states $|9, 0\rangle$ and $|9, 1\rangle$, and zero populations in the other states. At $t_1 = \frac{\pi}{3}/g_0^{\text{eff}} = 2.33 \times 10^{-7}$s, we obtain the state $|\psi_1\rangle = \frac{1}{2}|9, 0\rangle - i\frac{\sqrt{3}}{2}|9, 1\rangle$ with a fidelity of $F_1 = 0.9998$.

Step 2. We set $\Delta = 12\Omega$ to ensure almost ideal selective resonance between the states $|9, 1\rangle$ and $|9, 2\rangle$ as illustrated in Fig. 1 (b). After $t_2 = \frac{\pi}{2}/g_1^{\text{eff}} = 2.62 \times 10^{-7}$s, we obtain the state $|\psi_2\rangle = \frac{1}{2}e^{-i\phi_{0,2}}|9, 0\rangle - \frac{\sqrt{3}}{2}e^{-i\phi_2}|9, 2\rangle$ with a fidelity of $F_2 = 0.9992F_1$, where $\phi_{0,2} = -18\Omega t_2$ and $\phi_2 = -22\Omega t_2$.

Step 3. We next set $\Delta = 8\Omega$ to ensure selective resonance almost exclusively between the states $|9, 2\rangle$ and $|9, 3\rangle$ as indicated in Fig. 1 (c). After $t_3 = \frac{\pi}{2}/g_2^{\text{eff}} = 2.29 \times 10^{-7}$s, we obtain the state $|\psi_3\rangle = \frac{1}{2}e^{-i\phi_{0,3}}|9, 0\rangle + i\frac{\sqrt{3}}{2}e^{-i\phi_3}|9, 3\rangle$ with a fidelity of $F_3 = 0.9994F_2$, where $\phi_{0,3} = \phi_{0,2}$ and $\phi_3 = \phi_2 - 12\Omega t_3$.

Step 4. We subsequently set $\Delta = 4\Omega$ to ensure selective

Population	Without NA errors	With NA errors
$\lvert 9,0\rangle$	0.0001	0.0001
$\lvert 9,1\rangle$	0.9997	0.9988
$\lvert 9,2\rangle$	0.0002	0.0010
$\lvert 9,3\rangle$	≈ 0	≈ 0
$\lvert 9,4\rangle$	≈ 0	≈ 0
$\lvert 9,5\rangle$	≈ 0	≈ 0
$\lvert 9,6\rangle$	≈ 0	≈ 0
$\lvert 9,7\rangle$	≈ 0	≈ 0
$\lvert 9,8\rangle$	≈ 0	≈ 0
$\lvert 9,9\rangle$	≈ 0	≈ 0

TABLE I: The effect of non-adiabatic (NA) errors on the scheme when the system evolves initially from $\lvert 9,0\rangle$ by approximating the varying energy levels to constant ones.

resonance almost strictly between the states $\lvert 9,3\rangle$ and $\lvert 9,4\rangle$ as demonstrated in Fig. 1 (d). After $t_4 = \frac{\pi}{2}/g_3^{\text{eff}} = 2.14 \times 10^{-7}$s, we obtain the state $\lvert \psi_4\rangle = \frac{1}{2}e^{-i\phi_{0,4}}\lvert 9,0\rangle + \frac{\sqrt{3}}{2}e^{-i\phi_4}\lvert 9,4\rangle$ with a fidelity of $F_4 = 0.9994F_3$, where $\phi_{0,4} = \phi_{0,3} + 18\Omega t_4$ and $\phi_4 = \phi_3 - 6\Omega t_4$.

Step 5. We set $\Delta = 0$ to ensure selective resonance between the states $\lvert 9,4\rangle$ and $\lvert 9,5\rangle$ as exhibited in Fig. 1 (e). After $t_5 = \frac{\pi}{2}/g_4^{\text{eff}} = 2.09 \times 10^{-7}$s, we obtain the state $\lvert \psi_5\rangle = \frac{1}{2}e^{-i\phi_{0,5}}\lvert 9,0\rangle - i\frac{\sqrt{3}}{2}e^{-i\phi_5}\lvert 9,5\rangle$ with a fidelity of $F_5 = 0.9994F_4$, where $\phi_{0,5} = \phi_{0,4} + 36\Omega t_5$ and $\phi_5 = \phi_4 - 4\Omega t_5$.

Step 6. We finally set $\Delta = -4\Omega$ to ensure the approximately ideal selective resonance between the states $\lvert 9,5\rangle$ and $\lvert 9,6\rangle$ as presented in Fig. 1 (f). After $t_6 = \frac{\pi}{2}/g_5^{\text{eff}} = 2.14 \times 10^{-7}$s, we obtain the state $\lvert \psi_6\rangle = \frac{1}{2}e^{-i\phi_{0,6}}\lvert 9,0\rangle - \frac{\sqrt{3}}{2}e^{-i\phi_6}\lvert 9,6\rangle$ with a fidelity of $F_6 = 0.9994F_5$, where $\phi_{0,6} = \phi_{0,5} + 54\Omega t_6$ and $\phi_6 = \phi_5 - 6\Omega t_6$.

After the above six-step evolution which takes a time of $T = \sum_{i=1}^{6} t_i = 1.36 \times 10^{-6}$s, we obtain the state $\lvert \psi_6\rangle = \frac{1}{2}e^{-i\phi_{0,6}}\lvert 9,0\rangle - \frac{\sqrt{3}}{2}e^{-i\phi_6}\lvert 9,6\rangle$ with fidelity $F_6 \approx 0.997$. Note that $\lvert \psi_6\rangle$ lies within the code-space of a permutation-invariant code that corrects a single-qubit error, and corresponds to a local unitary transformation of the Ruskai code [16]. In particular, any subspace $\mathcal{C}$ spanned by the logical states $\lvert 0_L\rangle = \frac{1}{2}e^{-i\theta_1}\lvert 9,0\rangle - \frac{\sqrt{3}}{2}e^{-i\theta_2}\lvert 9,6\rangle$ and $\lvert 1_L\rangle = \frac{1}{2}e^{-i\theta_3}\lvert 9,9\rangle - \frac{\sqrt{3}}{2}e^{-i\theta_4}\lvert 9,3\rangle$ for any real numbers $\theta_1, \theta_2, \theta_3$ and θ_4 necessarily satisfies the quantum error correction criterion for a single-qubit error. To see this, we compare the code $\mathcal{C}$ with the Ruskai code that has logical codewords $\lvert R_0\rangle = \frac{1}{2}\lvert 9,0\rangle + \frac{\sqrt{3}}{2}\lvert 9,6\rangle$ and $\lvert R_1\rangle = \frac{1}{2}\lvert 9,9\rangle + \frac{\sqrt{3}}{2}\lvert 9,3\rangle$ [16, 17]. To show that $\mathcal{C}$ can correct a single-qubit error, it suffices to show that the Knill-Laflamme quantum error correction criterion

[1] which holds for the Ruskai code also holds for $\mathcal{C}$. This in turn is true because the matrix elements $\langle i_L\lvert P\rvert j_L\rangle$ are equivalent to $\langle R_i\lvert P\rvert R_j\rangle$ for all multi-qubit Pauli matrices that affect up to two qubits. Using the selective oscillation between two neighboring Dicke states as shown in Fig. 2, it is possible to achieve superpositions of Dicke states with amplitudes of arbitrary magnitudes via a multi-step system evolution. Therefore, a simple variation of the evolution times and the values of Δ used in our scheme can produce any state in the code-space $\mathcal{C}$ of the form $c_0\lvert 0_L\rangle + c_1\lvert 1_L\rangle$ for a priori known amplitudes c_0 and c_1. For arbitrary unknown amplitudes c_0 and c_1, it is also possible to create any state in the code-space $\mathcal{C}$ by resorting to a sequence of CNOT gates. Suppose initially we have state $c_0\lvert -\rangle + c_1\lvert +\rangle$. By adding in eight ancillary qubits prepared in state $\lvert -\rangle$, we have $c_0\lvert ---------\rangle + c_1\lvert +--------\rangle$. Applying a sequence of CNOT gates yields the state $c_0\lvert 9,0\rangle + c_1\lvert 9,9\rangle$. The CNOT gates can be implemented based on Hamiltonian (1) as shown in Refs. [10, 23]. Hence, by applying the above sequence of selective oscillations between neighboring Dicke states, we can obtain $c_0\lvert 0_L\rangle + c_1\lvert 1_L\rangle$, which is an arbitrary encoded state in the nine-qubit QECC. Thus, we can in principle encode any qubit holding our quantum data into a nine-qubit permutation-invariant code that corrects one error using the selective resonance interaction. Moreover, since our methodology can generate generic superpositions of Dicke states, we can also initialize any permutation-invariant quantum state in the code-space of any permutation-invariant quantum error correction code, where N can be in general larger than nine [17–20]. Although the minimum number of qubits required for a permutation-invariant code to correct one error is seven [21], we choose to use a nine-qubit permutation-invariant quantum code code to illustrate our methodology. This is because the nine-qubit permutation-invariant quantum code exhibits a robustness against phases appended onto the Dicke states of the code's logical codewords that the seven-qubit permutation-invariant quantum code need not have. In particular, when the phases for the seven-qubit permutation-invariant quantum code are perturbed, the resultant code may no longer be able to correct an arbitrary single-qubit error.

The implementation of our scheme can be possibly achieved with superconducting charge qubits which have been demonstrated to describe quantum spin models by resorting to a mutual inductance, a capacitance, or a LC resonator [24–28]. Given a system of identical charge qubits coupled by a common superconducting inductance, each charge qubit is a Cooper-pair box in which a superconducting island is weakly coupled by two symmetric dc superconducting quantum interference devices (SQUIDs) and biased by an applied voltage through a gate capacitance, and each SQUID is pierced by a magnetic flux. Therefore each qubit is controllable by the magnetic flux and the voltage applied via the gate capacitance. The system Hamiltonian is of the following

Fidelity	No noise	$\gamma_z = 10^{-3}\Omega$	$\gamma_z = 2 \times 10^{-3}\Omega$
F_1	0.9992	0.859	0.75
F_2	$0.9972F_1$	$0.753F_1$	$0.597F_1$
F_3	$0.997F_2$	$0.708F_2$	$0.534F_2$
F_4	$0.9972F_3$	$0.693F_3$	$0.514F_3$
F_5	$0.997F_4$	$0.689F_4$	$0.508F_4$
F_6	$0.9972F_5$	$0.693F_5$	$0.514F_5$

TABLE II: The effect of qubit dephasing on the performance of the generation of the 9-qubit QECC.

Fidelity	No noise	$\gamma_- = 10^{-3}\Omega$	$\gamma_- = 2 \times 10^{-3}\Omega$
F_1	0.9992	0.974	0.949
F_2	$0.9972F_1$	$0.933F_1$	$0.874F_1$
F_3	$0.997F_2$	$0.913F_2$	$0.837F_2$
F_4	$0.9972F_3$	$0.899F_3$	$0.812F_3$
F_5	$0.997F_4$	$0.884F_4$	$0.787F_4$
F_6	$0.9972F_5$	$0.869F_5$	$0.762F_5$

TABLE III: The effect of qubit relaxation on the performance of the generation of the 9-qubit QECC.

form [26],

$$H = \sum_i (\hbar\epsilon\sigma_z^i - \hbar\Delta\sigma_x^i) + \sum_{i,j} \hbar\Omega_{ij}\sigma_x^i\sigma_x^j. \quad (3)$$

The qubit parameters and qubit-qubit coupling strength in the Hamiltonian are adjustable. The Hamiltonian is of a similar form to Hamiltonian (1) with controllable parameters, and hence our scheme to initialize the QECC may be implementable in the system.

IV. THE EFFECT OF DECOHERENCE

In practice, decoherence due to the coupling of the system to the environment is inevitable. We discuss the performance of the quantum operations based on selective resonant interaction in the presence of noise. The evolution of the system is governed by the following master equation in the presence of noise,

$$\frac{d\rho}{dt} = -i[H,\rho] + \sum_{k=z,-} \gamma_k \left(\mathcal{L}_k\rho\mathcal{L}_k^\dagger - \frac{1}{2}\mathcal{L}_k^\dagger\mathcal{L}_k\rho - \frac{1}{2}\rho\mathcal{L}_k^\dagger\mathcal{L}_k \right) \quad (4)$$

where $\gamma_{z,-}$ are the decay rates of qubit dephasing and relaxation respectively, and $\mathcal{L}_z = \sum_{j=1}^9 \sigma_z^j$, $\mathcal{L}_- = \sum_{j=1}^9 \sigma_-^j$ where $\sigma_-^j = \frac{1}{2}(\sigma_x^j - i\sigma_y^j)$.

Given the above master equation describing the decoherence process, we can quantify the fidelities F_i ($i = 1, \cdots, 6$) of the generated states $|\psi_i\rangle$ using the selective

resonance transition in the presence of noise. The numerical results are listed in Tables II and III for different decay rates. The physical parameters are chosen as $\Omega/2\pi = 5 \times 10^8$Hz, $\epsilon = 0.06\Omega$, and Δ is changing step by step. We study how the dephasing and relaxation noise affect the performance of our scheme individually. We choose $\gamma_- = 0$ but vary γ_z firstly, and numerical results are shown in Table II. Next we select $\gamma_z = 0$ but vary γ_-, see Table III for details. It is illustrated by the numerical results that the gate fidelities are more robust against qubit relaxation than qubit dephasing. When the decay rates are increased, the gate fidelities are largely affected by the noise as compared with the fidelities in the absence of decoherence. This suggests that our scheme is vulnerable to large decay rates, which is expected from a scheme based on selective resonant interaction. The presence of the noise may affect the large detuning constraint and thereby result in imperfect selective resonant interaction.

V. THE SELECTIVE RESONANT INTERACTION FROM QUBIT-RESONATOR COUPLING

Our scheme can also be implemented using a system with N qubits coupled to a quantum harmonic oscillator with resonance frequency ω_r. The system's Hamiltonian is

$$H' = \sum_{j=1}^N \frac{\hbar\epsilon}{2}\sigma_z^j + \frac{\hbar\Delta}{2}\sigma_x^j + \hbar\omega_r a^\dagger a + \hbar g(a^\dagger + a)\sigma_x^j, \quad (5)$$

where a and $a^\dagger$ denote the bosonic ladder operators for the resonator, ϵ and Δ are the parameters describing the energy of each qubit, and g denotes the coupling strength between each qubit and the resonator. For simplicity, we take every qubit to be identical. Upon conjugating H' by a unitary transformation $U = \exp\left(-\frac{g}{\omega_r}\sum_{j=1}^N \left[(a^\dagger - a)\sigma_x^j\right]\right)$, we obtain the transformed Hamiltonian $\mathcal{H} = UH'U^\dagger$ with decomposition $\mathcal{H} = \mathcal{H}_0 + \mathcal{H}_I$. Here $\mathcal{H}_0$ and $\mathcal{H}_I$ denote Hamiltonians with and without qubit-resonator couplings respectively, where

$$\mathcal{H}_0 = \hbar\omega_r a^\dagger a + \sum_{j=1}^N \frac{\hbar\Delta}{2}\sigma_x^j - \sum_{j=1}^N\sum_{i=1}^{j-1} \frac{2\hbar g^2}{\omega_r}\sigma_x^i\sigma_x^j,$$

$$\mathcal{H}_I = \frac{\hbar\epsilon}{2}\sum_{j=1}^N \left(D(\frac{2g}{\omega_r})\frac{\sigma_z^j - i\sigma_y^j}{2} + D(-\frac{2g}{\omega_r})\frac{\sigma_z^j + i\sigma_y^j}{2} \right), \quad (6)$$

and $D(\alpha) = e^{\alpha(a^\dagger - a)}$ denotes the displacement operator.

Denoting $|\emptyset\rangle$ as the vacuum state of the resonator, one can easily show that $|N,n\rangle|\emptyset\rangle$ is an eigenstate of $\mathcal{H}_0$ with energy $\mathcal{E}_n = \frac{2n-N}{2}\hbar\Delta + \frac{\hbar g^2}{\omega_r}(N - 4n^2 + 4Nn - N^2)$.
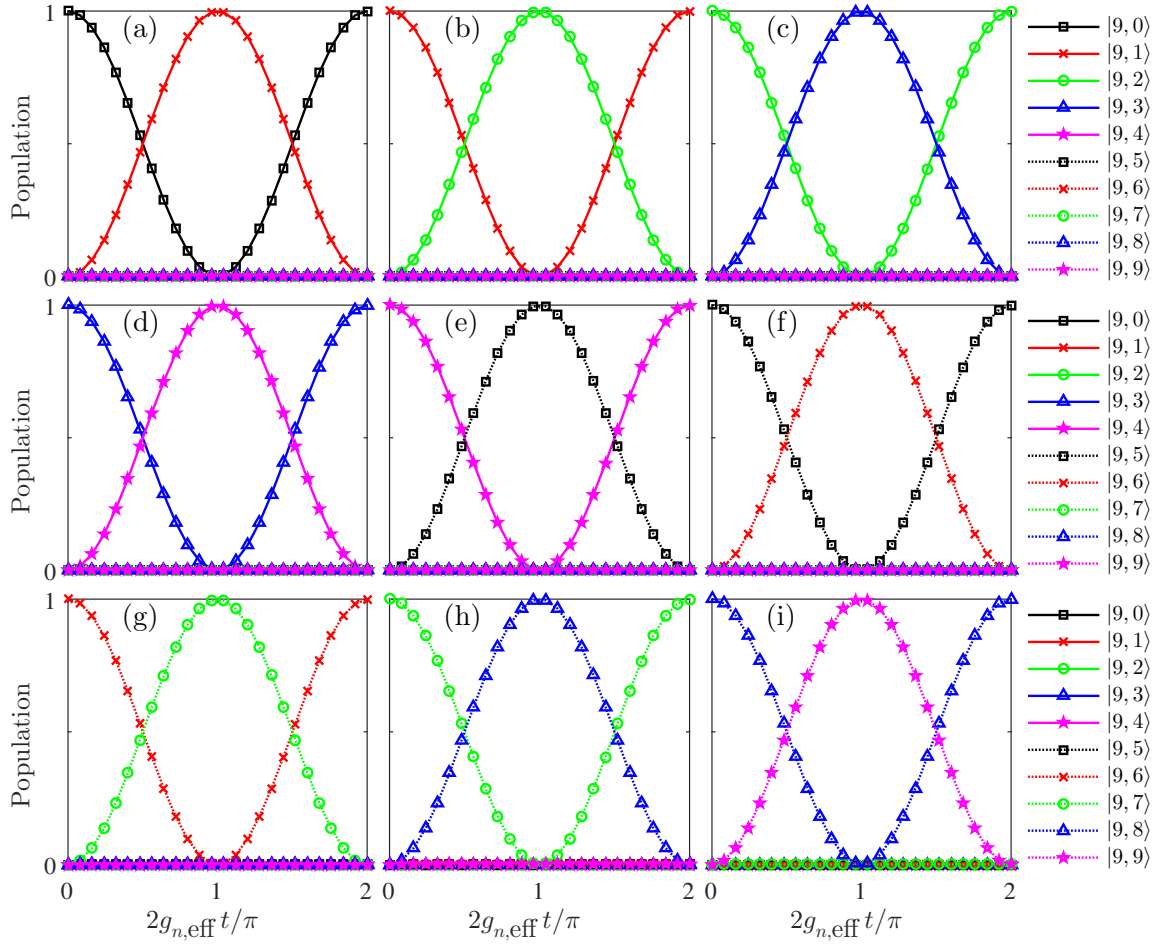
FIG. 2: Population of states $|9, n\rangle|\emptyset\rangle$ (where $n = 0, \cdots, 9$) with initial states prepared in (a) $|9, 0\rangle|\emptyset\rangle$, (b) $|9, 1\rangle|\emptyset\rangle$, (c) $|9, 2\rangle|\emptyset\rangle$, (d) $|9, 3\rangle|\emptyset\rangle$, (e) $|9, 4\rangle|\emptyset\rangle$, (f) $|9, 5\rangle|\emptyset\rangle$, (g) $|9, 6\rangle|\emptyset\rangle$, (h) $|9, 7\rangle|\emptyset\rangle$, and (i) $|9, 8\rangle|\emptyset\rangle$, respectively by properly choosing parameters. Time t's are dependent on $g_{n,\text{eff}}$ with $n = 0$ for (a), $n = 1$ for (b), $n = 2$ for (c), $n = 3$ for (d), $n = 4$ for (e), $n = 5$ for (f), $n = 6$ for (g), $n = 7$ for (h), and $n = 8$ for (i).

The energy gap $\mathcal{D}_n = \mathcal{E}_{n+1} - \mathcal{E}_n$ between two neighbouring energy levels can be written as $\mathcal{D}_n = \hbar\Delta + \frac{4\hbar g^2}{\omega_r}(N - 2n - 1)$. We consider case that $\mathcal{D}_{n_0} = 0$ for some n_0 and $\mathcal{D}_n \neq 0$ for all $n \neq n_0$, and in this case the effective coupling strengths of the transitions $|N, n\rangle|\emptyset\rangle \leftrightarrows |N, n + 1\rangle|\emptyset\rangle$ is of the following form $g_{n,\text{eff}} = \hbar\epsilon\sqrt{(N - n)(n + 1)}e^{-2g^2/\omega_r^2}/2$. Given the large detuning constraint that the energy gaps $\mathcal{D}_n$ are much larger than $g_{n,\text{eff}}$ for all $n \neq n_0$, the system's evolution is nothing but the selective resonant interaction,

$$\mathcal{H}_{\text{eff}} = g_{n_0,\text{eff}}\big(|N, n_0\rangle\langle N, n_0 + 1| \otimes |\emptyset\rangle\langle\emptyset| + |N, n_0 + 1\rangle\langle N, n_0| \otimes |\emptyset\rangle\langle\emptyset|\big), \quad (7)$$

since the other transitions corresponding to $n \neq n_0$ are dispersive. In the following, we neglect the resonator vacuum state since it can be decoupled from the qubit state.

With controllable parameters to implement the selective resonant interaction, a permutation-invariant QECC code may be generated in a broad coupling regime of light-matter interaction, including the weak, strong, and ultrastrong coupling regimes. In the following, we numerically describe the performance of the selective resonant interaction in the ultrastrong coupling regime. Let the system evolve from different initial states by fixing the parameters $g = 1/8\omega_r$, $\epsilon = 0.001\omega_r$ and $\omega_r = 2\pi \times 1$ GHz while adjusting Δ. The numerical results are summarized in Fig. 2. It is clearly demonstrated that we have obtained nearly perfect oscillations between the neighbouring states, and therefore the initialization of the QECC can be achieved with excellent fidelities in the system. We can obtain $|\psi_i'\rangle$ with $i = 1, \cdots, 6$ (which are different from $|\psi_i\rangle$ in phases) numerically, and eventually obtain $|\psi_6'\rangle$ with a fidelity of $F_6' \approx 0.996$ and total evolution time $T' = 6.7 \times 10^{-7}$s.

The Hamiltonian in Eq.(5) with adjustable ϵ and Δ can be naturally implemented in the circuit QED systems with charge and flux qubits. The flux qubits, which have been demonstrated to be capable of reaching the ultrastrong and deep strong coupling regimes [29–31], may

require less gate operation time. However, it is hard to implement our QECC scheme since the g and Δ cannot be individually adjusted to satisfy the large detuning constraint [32, 33]. Nevertheless, it is possible to implement our QECC scheme in the circuit QED systems with superconducting charge qubits working in the strong coupling regime [33–35].

We consider the case with 9 charge qubits placed at the antinodes of the magnetic field induced by the oscillating supercurrent in the transmission line resonator (TLR), as shown in Fig. 3. Each charge qubit comprises of a dc superconducting quantum interference device (SQUID) formed by a superconducting island connected to two Josephson junctions. In this situation, the external magnetic flux threading the j-th dc-SQUID Φ_e^j is the sum of the classically-applied magnetic flux Φ_{e0}^j and the quantized magnetic flux induced by the TLR Φ_r^j [33–35]. By expanding the Josephson energy to linear order in $\pi \Phi_r^j / \Phi_0$, where $\Phi_0 = h/2e$ is the magnetic-flux quantum, we attain the linear interaction between the charge qubits and the quantized field of the TLR. The total Hamiltonian is then [33, 35]

$$H = \sum_{j=1}^{N} \frac{E_C^j}{4}(2n_g^j - 1)\sigma_z^j - E_J^j \cos\left(\pi \frac{\Phi_{e0}^j}{\Phi_0}\right)\sigma_x^j$$
$$+ \hbar\omega_r a^\dagger a + \sum_{j=1}^{N} \hbar g^j (a^\dagger + a)\sigma_x^j, \qquad (8)$$

where E_C^j (E_J^j) is the Coulomb (Josephson) energy of the jth qubit, Φ_e^j is the external magnetic flux, $n_g^j = C_g^j V_g^j / 2$ is the bias charge number which can be controlled by the gate voltage V_g^j, and C_g^j is the gate capacitor. The Pauli matrices of the j-th qubit $\sigma_z^j = |1^j\rangle\langle 1^j| - |0^j\rangle\langle 0^j|$ and $\sigma_x^j = |0^j\rangle\langle 1^j| + |1^j\rangle\langle 0^j|$ are defined in terms of the charge eigenstates $|1^j\rangle$ and $|0^j\rangle$, which denote 0 and 1 excess Cooper pair on the corresponding island, respectively. The coupling parameter is [33, 35]

$$g^j = \pi \frac{S_0^j E_J}{d\Phi_0}\sqrt{\frac{l\omega_r}{\hbar L_0}}\sin\left(\pi \frac{\Phi_{e0}^j}{\Phi_0}\right), \qquad (9)$$

where S_0^j is the enclosed area of the dc-SQUID, l is the inductance per unit length, L_0 is the geometric length of the TLR, d is the distance between the qubit and the transmission line. From Eq. (8), the free charge qubit can be controlled by both the gate voltage and the external magnetic fluxes. The coupling parameter g^j is also adjustable through the applied magnetic flux. For simplicity and without loss of generality, we assume all the charge qubits to be identical so that $C_g^j = C_g$, $E_J^j = E_J$, $E_C^j = E_C$. We choose the following experimentally accessible parameters [34–36]: $S_0/d \approx 100\,\mu m$, $E_J \approx 110\,\mu eV$, $L_0 \approx 1.5$ cm, $l \approx 2\times 10^{-6}$ Hm^{-1}, $\omega_r \approx 2\pi\times 1$ GHz, which results in a maximized normalized coupling strength of $g_{max}/\omega_r = g_{max}^j/\omega_r \approx 0.0382$.
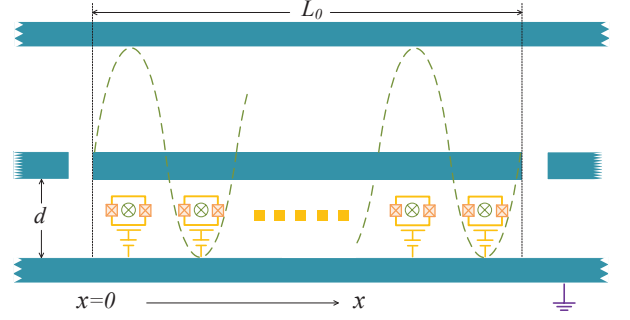

FIG. 3: Schematic of circuit QED design to generate the permutation-invariant QECC code. An array of charge qubits array are placed inside a transmission line resonator.

Since Eq. (8) has the same form as Hamiltonian (5) with $\epsilon = \frac{E_C}{2}(2n_g - 1)$, $\Delta = -2E_J\cos\theta$, and $g = g_{max}\sin\theta$ where $\theta/\pi = \frac{\Phi_{e0}^j}{\Phi_0}$, we can use the six-step evolution mentioned earlier to create the QECC in this physical system with strong qubit-resonator couplings by choosing $\epsilon = 0.0004\omega_r$, $\omega_r = 2\pi \times 1$ GHz and varying θ. We find $|\psi_i''\rangle$ with $i = 1, \cdots, 6$ (which are different from $|\psi_i\rangle$ and $|\psi_i'\rangle$ in phases) with the corresponding θ, and thus $|\psi_6''\rangle$ with a fidelity of $F_6'' = 0.92$ and total evolution time is $T'' = 1.64 \times 10^{-6}$s. With the strong qubit-resonator coupling, the required evolution time is slightly increased and fidelity is reduced as expected. According to our scheme, further increase in fidelity and decrease in operation time is possible if Δ and ϵ were to be tunable with stronger qubit-resonator coupling. These improvements that require achievable stronger qubit-resonator coupling and adjustable parameters in Hamiltonian await further theoretical and experimental advances.

VI. CONCLUSION

To summarize, we have presented a scheme to create a nine-qubit permutation-invariant QECC in two physical systems by resorting to the selective resonant interaction. Firstly we considered a system of qubits coupled to each other. It is possible to create the nine-qubit QECC in nanoseconds with very high fidelity via six-step evolution of the system. With the aid of single/two-qubit operations, any state in the code-space $\mathcal{C}$ with unknown amplitudes can be generated based on the selective resonant interaction. Our results pave a promising way toward achieving fast generation of the multi-qubit QECC and thus reduce the errors incurred at the level of creating QECC. The effect of decoherence on our scheme has been explored and we found that our scheme is largely affected when the decay rate of noise is increasing. To ensure the excellent performance of our scheme, small decoherences are preferred.

The selective resonant interaction can also be derived in a system of qubits coupled to a quantum resonator.

Upon a unitary transformation, the transformed system Hamiltonian is just the selective resonant interaction. In our scheme the large detuning constraint of the selective resonant interaction is crucial and the constraint can be fulfilled with controllable system parameters. With adjustable parameters to implement the selective resonant interaction, the nine-qubit QECC may be initialized in a broad coupling regime of light-matter interaction. In the ultrastrong coupling regime, the evolution time can be further reduced and fidelity can be improved as expected. These improvements await future advances in both theory and experiment.

We would appreciate the valuable suggestions from

[1] E. Knill and R. Laflamme, Phys. Rev. A **55**, 900 (1997).
[2] A. M. Steane, Phys. Rev. Lett. **77**, 793 (1996).
[3] P. W. Shor, Phys. Rev. A **52**, R2493 (1995).
[4] A. Kitaev, Ann. Phys. **303**, 2, (2003).
[5] M. A. Nielsen, I. L. Chuang, Quantum Computation and Quantum Information.
[6] J. Chiaverini, D. Leibfried, T. Schaetz, M. D. Barrett, R. B. Blakestad, J. Britton, W.M. Itano, J. D. Jost, E. Knill, C. Langer, R. Ozeri, and D. J. Wineland, Nature, **432**, 602 (2004).
[7] C.-Y. Lu, W.-B. Gao, J. Zhang, X.-Q. Zhou, T. Yang, J.-W. Pan, Proc. Natl. Acad. Sci. **105**, 11050 (2008).
[8] M. D. Reed, L. DiCarlo, S. E. Nigg, L. Sun, L. Frunzio, S. M. Girvin, and R. J. Schoelkopf, Nature, **482**, 382 (2012).
[9] B. A. Bell, D. A. Herrera-Martí, M. S. Tame, D. Markham, W. J. Wadsworth, and J. G. Rarity, Nature Comm. **5**, 3658 (2013).
[10] T. H. Kyaw, D. A. Herrera-Martí, E. Solano, G. Romero, and L.-C. Kwek, Phys. Rev. B **91**, 064503 (2015).
[11] Y.-F. Xiao, X.-B. Zou, and G.-C. Guo, Phys. Rev. A **75**, 012310 (2007).
[12] L. B. Yu, Z.-Y. Xue, Z. D. Wang, Y. Yu, and S. L. Zhu, Eur. Phys. J. D **61**, 499 (2011).
[13] Z.-Y. Xue and S. Liu, J. Mod. Opt. **60**, 474 (2013).
[14] C. Wu, C. Guo, Y. Wang, G. Wang, X.-L. Feng, and J.-L. Chen, Phys. Rev. A **95**, 013845 (2017).
[15] F. Armata, G. Calajo, T. Jaako, M. S. Kim, and P. Rabl, Phys. Rev. Lett. **119**, 183602 (2017).
[16] M. B. Ruskai, Phys. Rev. Lett. **85**, 194 (2000).
[17] Y. Ouyang, Phys. Rev. A, **90**, 062317 (2014).
[18] Y. Ouyang and J. Fitzsimons, Phys. Rev. A **93**, 042340 (2016).
[19] Y. Ouyang, Linear Algebra Appl. **532**, 43 (2017).
[20] Y. Ouyang, arXiv preprint, arXiv:1809.09801 (2018).

[21] H. Pollatsek and M. B. Ruskai, Linear Algebra Appl. **392**, 255 (2004).
[22] K. Saito, M. Wubs, S. Kohler, Y. Kayanuma, and P. Hänggi, Phys. Rev. B **75**, 214308 (2007).
[23] J. Zhang, S. J. Devitt, J. Q. You, and F. Nori, Phys. Rev. A **97**, 022335 (2018).
[24] Y. Makhlin, G. Schön, and A. Shnirman, Nature **398**, 305 (1999).
[25] F. Marquardt and C. Bruder, Phys. Rev. B **63**, 054514 (2001).
[26] J. Q. You, J. S. Tsai, and F. Nori, Phys. Rev. Lett. **89**, 197902 (2002).
[27] Y. A. Pashkin, T. Yamamoto, O. Astafiev, Y. Nakamura, D. V. Averin, and J. S. Tsai, Nature **421**, 823 (2003).
[28] J. Q. You, X.-F. Shi, X. Hu, and F. Nori, Phys. Rev. B **81**, 014505 (2010).
[29] P. Forn-Díaz, J. J. García-Ripoll, B. Peropadre, J.-L. Orgiazzi, M. A. Yurtalan, R. Belyansky, C. M. Wilson, and A. Lupascu, Nat. Phys. **13**, 39 (2017).
[30] F. Yoshihara, T. Fuse, S. Ashhab, K. Kakuyanagi, S. Saito, and K. Semba, Nat. Phys. **13**, 44 (2017).
[31] Z. Chen, Y. Wang, T. Li, L. Tian, Y. Qiu, K. Inomata, F. Yoshihara, S. Han, F. Nori, J. S. Tsai, and J. Q. You, Phys. Rev. A **96**, 012325 (2017).
[32] Y.-D. Wang, A. Kemp, and K. Semba, Phys. Rev. B **79**, 024502 (2009).
[33] Y.-D. Wang, S. Chesi, D. Loss, and C. Bruder, Phys. Rev. B **81**, 104524 (2010).
[34] Y. D. Wang, Z. D. Wang, and C. P. Sun, Phys. Rev. B **72**, 172507 (2005).
[35] Y.-M. Wang and C.-Z. Li, Commun. Theor. Phys. **53**, 190 (2010).
[36] G. Chen, Z. Chen, and J. Liang, Phys. Rev. A **76**, 055803 (2007).